CHAPTER IV

APPLICATION OF STOCHASTIC SIMULATION IN PERMEABILITY EQUATION DETERMINATION

Estimation of permeability in uncored but logged well is a generic problem common to all reservoirs. For this study, porosity plays an important role when estimating permeability on uncored wells. In this chapter, each section discusses the determination of permeability equation from porosity. In addition, two realization maps of porosity with their corresponding calculated permeability and porosity and permeability from core analysis will be used as inputs in reservoir simulation program. The variation of production profiles can then be observed.

4.1 Data Preview for Estimating Permeability Equation

As mentioned in Chapter 1, permeability measurement from core analysis is a direct measurement provided more accurate result than other indirect measurements. As a result, permeability and porosity from core analysis are used for estimating permeability equation. Table 4.1 shows permeability and porosity from core analysis. The porosity data generated from Sequential Gaussian Simulation at the same depth of permeability measurement is shown in Table 4.2.

Table 4.1: Permeability measurement from core analysis.

Layer	Depth (m)	Permeability (md)	Porosity
K2	1,620.5	658	0.258
K2	1,626.2	2,420	0.281
K2	1,636.0	51	0.219
K3	1,646.2	2,100	0.264
K3	1,646.6	533	0.243
K3	1,647.1	1,760	0.264
K3	1,648.0	2,560	0.269
Mean		1,440	0.257

Table 4.2: Porosity from simulation at the same depth of core analysis.

Layer	Depth (m)	Porosity	Simulated Porosity	Realization
K2	1,620.5	0.258	0.209	1
			0.190	2
			0.182	3
			0.203	4
			0.182	5
			0.182	6
			0.203	7
			0.203	8
			0.182	9
			0.182	10
			0.182	11
			0.203	12
			0.182	13
			0.203	14
			0.190	15
			0.182	16
	1,626.2	0.281	0.212	1
			0.212	2
			0.209	3
			0.212	4
			0.203	5
			0.212	6
			0.212	7
			0.209	8
			0.2105	9
			0.2105	10
			0.212	11
			0.215	12
			0.203	13
			0.212	14
			0.212	15
			0.209	16
	1,636.0	0.219	0.221	1
			0.221	2
			0.221	3
			0.221	4
			0.215	5
			0.182	6

Table 4.2: Porosity from simulation at the same depth of core analysis (continued).

Layer	Depth (m)	Porosity	Simulated Porosity	Realization
K2	1,636.0	0.219	0.221	7
			0.221	8
			0.218	9
			0.218	10
			0.218	11
			0.221	12
			0.218	13
			0.218	14
			0.218	15
			0.218	16
K3	1,646.2	0.264	0.190	1
			0.166	2
			0.178	3
			0.169	4
			0.178	5
			0.174	6
			0.180	7
			0.169	8
			0.165	9
			0.178	10
			0.178	11
			0.166	12
			0.169	13
			0.180	14
			0.169	15
			0.212	16
	1,646.6	0.243	0.174	1
			0.168	2
			0.180	3
			0.168	4
			0.174	5
			0.171	6
			0.178	7
			0.169	8
			0.166	9
			0.174	10
			0.166	11
			0.169	12

Table 4.2: Porosity from simulation at the same depth of core analysis (continued).

Layer	Depth (m)	Porosity	Simulated Porosity	Realization
K3	1,646.6	0.243	0.166	13
			0.174	14
			0.169	15
			0.210	16
	1,647.1	0.264	0.171	1
			0.165	2
			0.174	3
			0.165	4
			0.168	5
			0.169	6
			0.171	7
			0.169	8
			0.168	9
			0.169	10
			0.169	11
			0.162	12
			0.165	13
			0.172	14
			0.166	15
			0.206	16
	1,648.0	0.269	0.168	1
			0.160	2
			0.168	3
			0.158	4
			0.169	5
			0.165	6
			0.169	7
			0.162	8
			0.162	9
			0.163	10
			0.162	11
			0.160	12
			0.160	13
			0.165	14
			0.166	15
			0.169	16

In Table 4.1, there are seven permeability values, including three permeability values in K2 layer and four permeability values in K3 layer located within the oil field. It was observed that the range of porosity does not have significant difference, contrary to permeability which displays a very wide range of data.

Table 4.2 shows 16 realizations of simulated porosity in each depth of permeability measurement. It was found that the range of porosity in each depth is not significantly different.

It is important to note that there is significant difference in the mean values between the core-measured porosity and simulated porosity. The mean porosity obtained from core analysis is 0.257, while the mean porosity obtained from simulated data is 0.186. The difference in pore volume of the reservoir will have significant impact on its production operation.

4.2 Permeability Equation Determination

The scatter plot of permeability and porosity is a good representative of the relationship between permeability and porosity. The scatter plot of permeability and porosity from core analysis is shown in Figure 4.1.

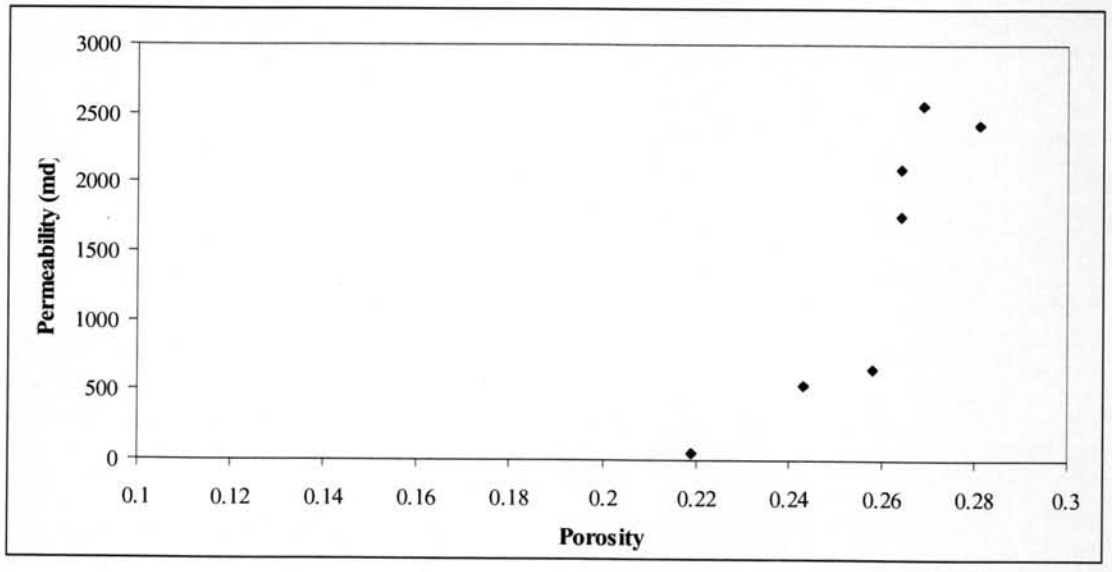

Figure 4.1: Scatter plot of permeability vs. porosity from core analysis.

A total of 7 data points in Figure 4.1 shows a scatter pattern that could be attributed to the existence of more than one rock type, a similar observation can be made for fluid flow properties. As mentioned earlier, the lithologies of the oil field consist of alternative clastic sediment layers of sandstone and claystone, but mineralogy (type, abundance, and location) and texture (grain size, grain shape, sorting, and packing) are probably different. Thus, the porosity-permeability relationship is best achieved if rocks with similar fluid-flow properties are identified and grouped together. Each group is referred to hydraulic flow unit.

Hydraulic flow unit was used in log-log plot of reservoir quality index (RQI) versus ratio of pore volume to grain volume (Φ_z) to estimate flow zone indicator (F_{zi}). Table 4.3 presents reservoir quality index and ratio of pore volume to grain volume values. Log-log plot of reservoir quality index (RQI) versus ratio of pore volume to grain volume (Φ_z) is shown in Figure 4.2.

Table 4.3: Reservoir quality index and ratio of pore volume to grain volume values.

Layer	Depth (m)	Permeability (md)	Porosity	Φz $\Phi/(1-\Phi)$	RQI $0.0314(k/\Phi)^{0.5}$
K2	1620.5	658	0.258	0.3477	1.5857
K2	1626.2	2420	0.281	0.3908	2.9140
K2	1636	51	0.219	0.2804	0.4792
K3	1646.2	2100	0.264	0.3587	2.8005
K3	1646.6	533	0.243	0.3210	1.4706
K3	1647.1	1760	0.264	0.3587	2.5638
K3	1648	2560	0.269	0.3680	3.0632

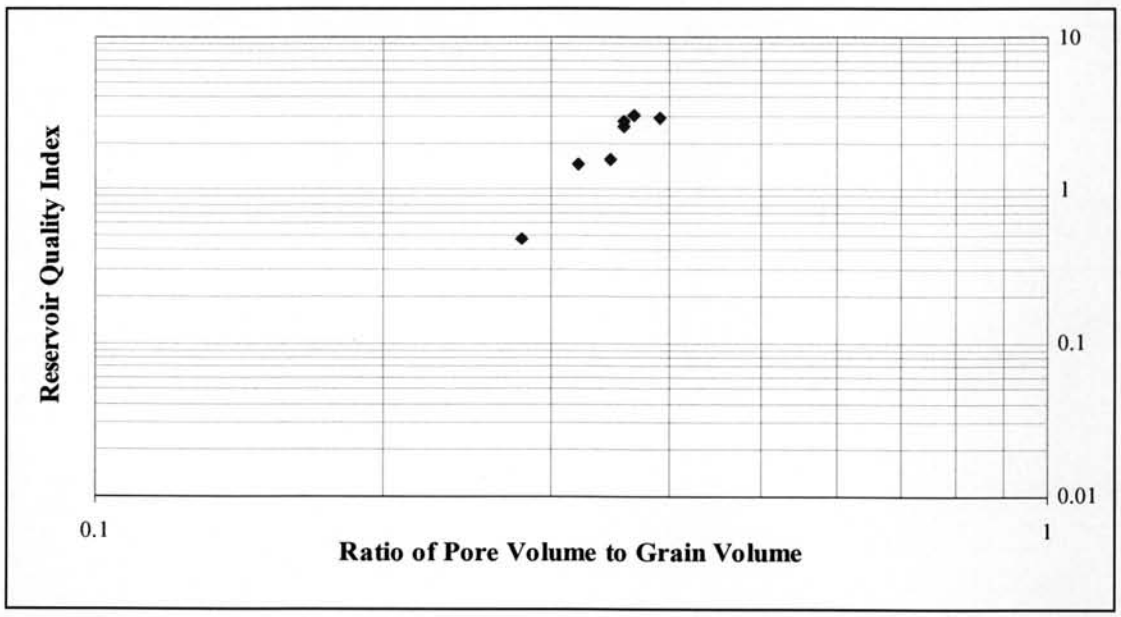

Figure 4.2: Log-log plot of RQI versus Φ_z.

From Figure 4.2, the plot shows a scatter pattern of data points rendering the classification of flow zone indicator impossible. As alternative approaches, histogram analysis and probability plot were used for flow zone indicator classification. The log F_{zi} histogram is shown in Figure 4.3.

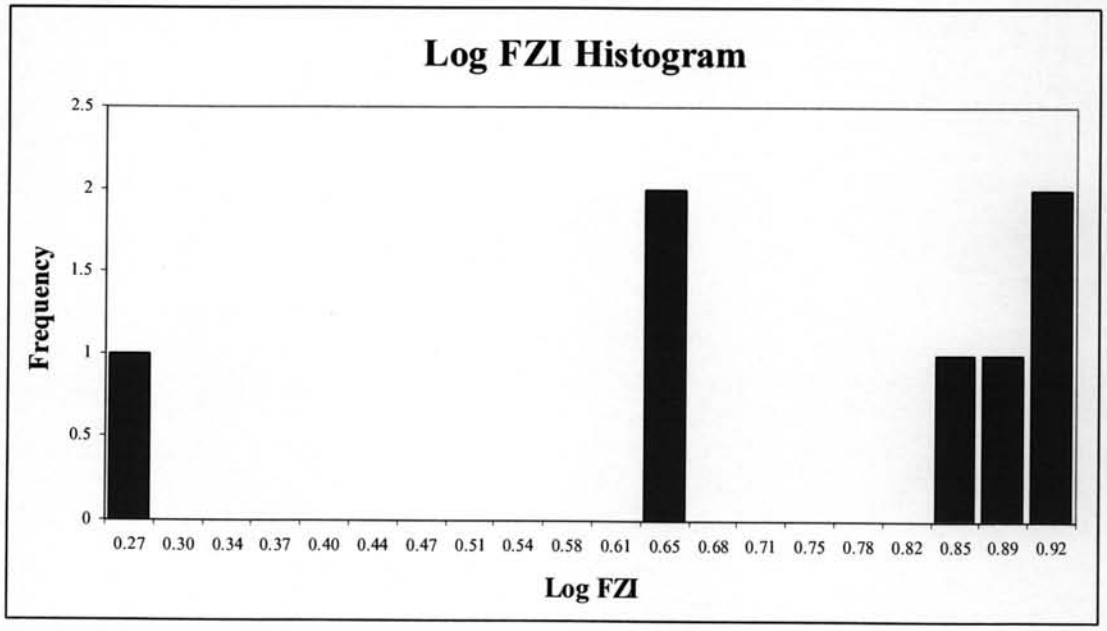

Figure 4.3: Histogram of Log F_{zi}.

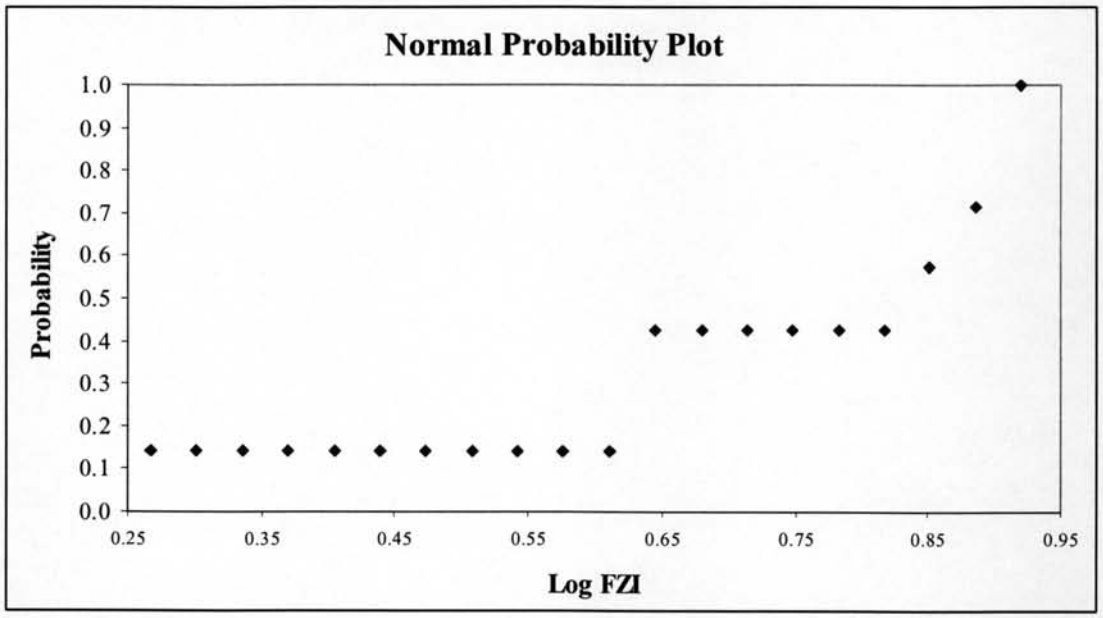

Figure 4.4: Normal probability plot of Log F_{zi}

Figure 4.3 indicates three groups of data. Thus, in order to corroborate and define the boundaries of each group, it is necessary to construct a probability plot as shown in Figure 4.4. The normal probability plot identifies and denotes three groups of hydraulic flow units. Based on the hydraulic flow unit definitions obtained from histogram analysis and probability plot, a combined RQI versus Φ_z plot was made and is shown in Figure 4.5. Table 4.4 is the classification of the hydraulic flow units according to clustering of log F_{zi}. The mean value for each group and the corresponding intervals are also presented.

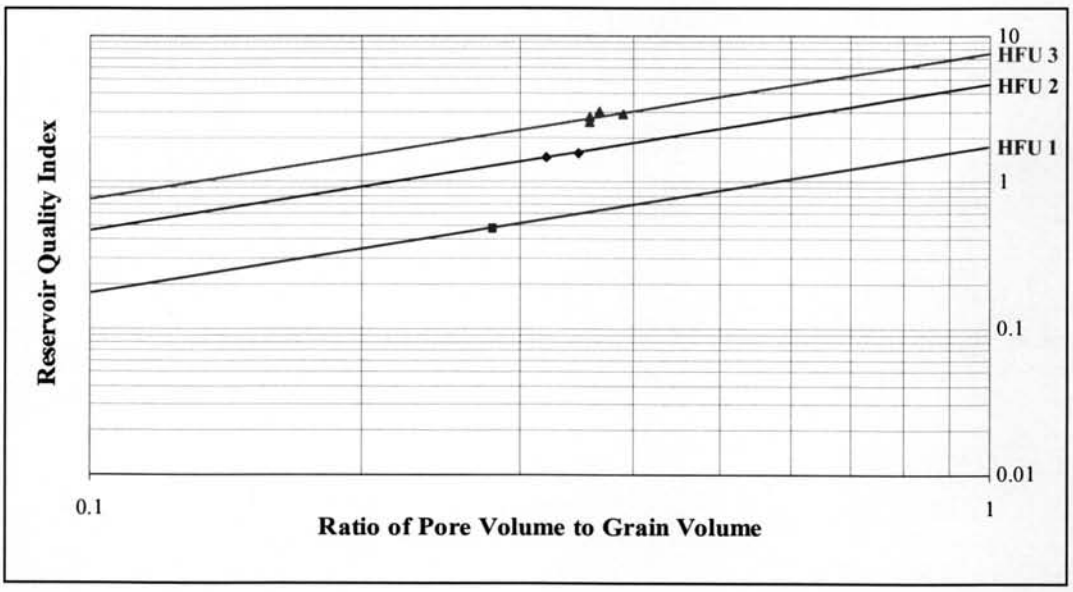

Figure 4.5: Hydraulic flow unit delineation

Table 4.4: The classification of the HFUs as Log F_{zi} interval and mean F_{zi}.

Unit or Group	Log Fzi Interval	Mean Fzi
1	0.233 - 0.233	1.71
2	0.659 - 0.661	4.57
3	0.854 - 0.920	7.67

Using the mean F_{zi}, the permeability determination equation can be tabulated for each HFU, their relationships are shown in Table 4.5.

Table 4.5: The classification of the hydraulic flow units as permeability eqation.

Unit or Group	Permeability Equation $k = 1014*(F_{zi\ mean})^2 * \frac{\Phi^3}{(1-\Phi)^2}$
1	$k = 1014*1.71^2* \frac{\Phi^3}{(1-\Phi)^2}$
2	$k = 1014*4.57^2 * \frac{\Phi^3}{(1-\Phi)^2}$
3	$k = 1014*7.67^2 * \frac{\Phi^3}{(1-\Phi)^2}$

Generally, logging attributes such as Gamma Rays, porosity from density log, porosity from neutron log, resistivity, and etc. are considered in selecting a permeability equation. But, this information is not available in this study. Therefore, the process of selecting permeability equation is solely based on data locations.

There are three permeability equations for this study. To confirm that these permeability equations are able to estimate permeability in this field, porosity from well logging data and simulated porosity were used to determine permeability from these equations. The permeability determination from simulated porosity and porosity of well logging data are shown in Tables 4.6 and 4.7, respectively. Figure 4.6 shows the log-log plot of RQI and Φz for porosity from well logging data, simulated porosity, and core analysis.

Table 4.6: Permeability determination from simulated porosity.

Layer	Depth	Porosity	Permeability (md)
K2	1,620.5	0.209	309
		0.19	221
		0.182	191
		0.203	279
		0.182	191
		0.182	191
		0.203	279
		0.203	279
		0.182	191
		0.182	191
		0.182	191
		0.203	279
		0.182	191
		0.203	279
		0.19	221
		0.182	191
	1,626.2	0.212	915
		0.212	915
		0.209	870
		0.212	915
		0.203	786
		0.212	915
		0.212	915
		0.209	870
		0.2105	893
		0.2105	893
		0.212	915
		0.215	962
		0.203	786
		0.212	915
		0.212	915
		0.209	870
	1,636.0	0.221	53
		0.221	53
		0.221	53
		0.221	53
		0.215	48
		0.182	27

Table 4.6: Permeability determination from simulated porosity (continued).

Layer	Depth	Porosity	Permeability (md)
K2	1,636.0	0.221	53
		0.221	53
		0.218	50
		0.218	50
		0.218	50
		0.221	53
		0.218	50
		0.218	50
		0.218	50
		0.218	50
K3	1,646.2	0.19	624
		0.166	392
		0.178	498
		0.169	417
		0.178	498
		0.174	461
		0.18	517
		0.169	417
		0.165	384
		0.178	498
		0.178	498
		0.166	392
		0.169	417
		0.18	517
		0.169	417
		0.212	915
	1,646.6	0.174	461
		0.168	409
		0.18	517
		0.168	409
		0.174	461
		0.171	434
		0.178	498
		0.169	417
		0.166	392
		0.174	461
		0.166	392
		0.169	417

Table 4.6: Permeability determination from simulated porosity (continued).

Layer	Depth	Porosity	Permeability (md)
K3	1,646.6	0.166	392
		0.174	461
		0.169	417
		0.21	885
	1,647.1	0.171	434
		0.165	384
		0.174	461
		0.165	384
		0.168	409
		0.169	417
		0.171	434
		0.169	417
		0.168	409
		0.169	417
		0.169	417
		0.162	361
		0.165	384
		0.172	443
		0.166	392
		0.206	827
	1,648.0	0.168	409
		0.16	346
		0.168	409
		0.158	332
		0.169	417
		0.165	384
		0.169	417
		0.162	361
		0.162	361
		0.163	369
		0.162	361
		0.16	346
		0.16	346
		0.165	384
		0.166	392
		0.169	417

Table 4.7: Permeability determination from porosity of well logging data.

Layer	Depth	Porosity	Permeability (md)
K2	1,530.35	0.170	151
	1,509.67	0.220	371
	1,551.33	0.210	314
	1,572.51	0.210	314
	1,554.30	0.200	265
	1,579.47	0.220	371
	1,604.73	0.200	265
	1,566.94	0.200	265
	1,590.08	0.210	314
	1,613.27	0.180	184
	1,625.25	0.190	624
	1,563.62	0.170	151
	1,588.79	0.160	123
	1,614.00	0.210	314
	1,601.73	0.170	151
	1,629.05	0.180	517
	1,587.43	0.170	151
	1,609.49	0.120	47
	1,631.77	0.240	507
	1,614.64	0.150	99
	1,636.01	0.140	11
	1,657.28	0.250	1,657
	1,678.64	0.260	1,915
	1,499.68	0.210	314
	1,517.11	0.160	346
	1,534.67	0.210	314
	1,525.37	0.200	265
	1,544.78	0.230	435
	1,564.22	0.150	99
	1,579.86	0.270	782
	1,552.93	0.160	123
	1,587.36	0.170	151
	1,606.83	0.190	221
	1,626.31	0.200	746
	1,604.42	0.180	184
	1,627.82	0.230	1,224

Table 4.7: Permeability determination from porosity of well logging data (contined).

Layer	Depth	Porosity	Permeability (md)
K3	1,616.21	0.190	624
	1,594.14	0.200	746
	1,638.27	0.150	14
	1,660.30	0.150	279
	1,630.10	0.130	173
	1,655.57	0.200	746
	1,681.17	0.230	1,224
	1,636.49	0.210	44
	1,659.81	0.130	173
	1,683.19	0.240	1,428
	1,705.90	0.160	346
	1,706.69	0.160	346
	1,639.42	0.180	517
	1,664.93	0.110	100
	1,690.59	0.190	624
	1,683.99	0.230	1,224
	1,711.53	0.200	746
	1,739.06	0.160	346
	1,676.74	0.140	221
	1,699.36	0.120	133
	1,722.09	0.210	885
	1,700.04	0.180	517
	1,743.46	0.200	746
	1,765.46	0.220	1,044
	1,787.69	0.150	279
	1,570.64	0.190	624
	1,594.02	0.090	53
	1,583.57	0.210	885
	1,620.31	0.140	221
	1,660.41	0.130	173
	1,680.41	0.180	517
	1,654.10	0.110	100
	1,645.74	0.230	1,224
	1,703.69	0.150	279
	1,722.70	0.200	746
	1,721.56	0.280	2,526
	1,745.23	0.150	279

Table 4.7: Permeability determination from porosity of well logging data (contined).

Layer	Depth	Porosity	Permeability (md)
K4	1,682.58	0.150	279
	1,704.96	0.200	746
	1,706.88	0.200	746
	1,732.69	0.180	517
	1,758.52	0.180	517
	1,784.46	0.150	279
	1,730.30	0.220	1,044
	1,753.99	0.190	624
	1,777.79	0.140	221
	1,780.18	0.220	1,044
	1,801.75	0.220	1,044
	1,742.31	0.160	346
	1,768.24	0.180	517
	1,766.61	0.120	133
	1,794.16	0.140	221
	1,821.75	0.200	746
	1,767.73	0.200	746
	1,790.66	0.170	425
	1,813.73	0.180	517
	1,810.13	0.170	425
	1,832.69	0.290	2,886
	1,855.41	0.240	1,428
	1,661.98	0.240	1,428
	1,679.23	0.230	1,224
	1,696.40	0.220	1,044
	1,714.81	0.200	746
	1,720.38	0.110	100
	1,740.06	0.180	517
	1,779.60	0.180	517
L2	1,769.71	0.220	1,044
	1,873.93	0.170	425
	1,875.44	0.130	173
	1,897.96	0.180	517
	1,846.29	0.150	279
	1,872.42	0.190	624
	1,924.88	0.310	3,733
	1,898.60	0.180	517
	1,883.46	0.190	624

Table 4.7: Permeability determination from porosity of well logging data (contined).

Layer	Depth	Porosity	Permeability (md)
L2	1,906.93	0.130	173
	1,925.09	0.310	3,733
	1,948.99	0.250	1,657
	1,749.15	0.220	1,044
	1,772.82	0.140	221
	1,839.36	0.120	133
	1,794.31	0.150	279
	1,914.96	0.150	279
	1,939.69	0.170	425
L3	1,790.15	0.140	221
	1,810.00	0.200	746
	1,829.01	0.170	425
	1,887.91	0.200	746
	1,913.64	0.180	517
	1,939.31	0.280	2,526
	1,922.24	0.170	425
	1,995.88	0.220	1,044
	1,997.72	0.230	1,224
	1,952.60	0.150	279
	1,960.41	0.150	279
	1,988.30	0.210	885
	1,930.64	0.170	425
	1,954.53	0.110	100
	1,973.18	0.360	6,795
	1,997.55	0.180	517
	2,022.11	0.170	425
	2,046.83	0.200	746
	1,814.14	0.210	885
	1,835.55	0.140	221
	1,879.76	0.200	746
	1,960.14	0.200	746
	1,914.66	0.100	74
	1,953.70	0.170	425
	1,973.26	0.160	346
	1,965.11	0.170	425
	2,042.03	0.140	221

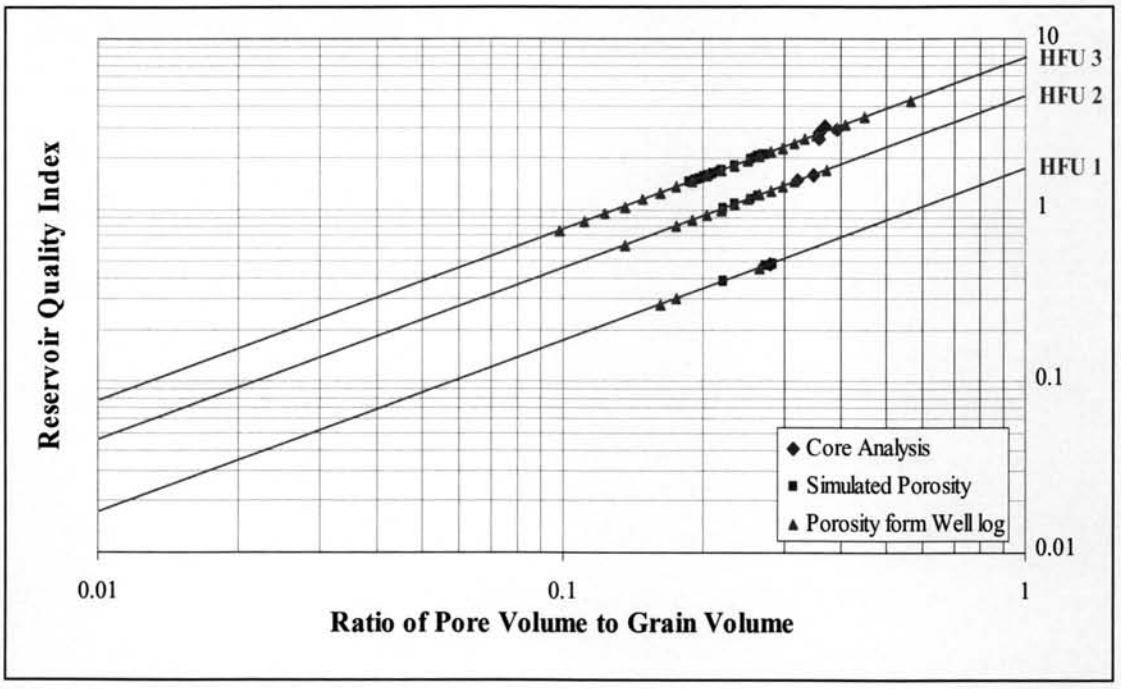

Figure 4.6: Log-log plot of RQI and Φz for porosity from well logging data, simulated porosity, and core analysis.

The permeability values estimated from equations in Table 4.5 using simulated and well log porosity as inputs provide the RQI and Φ_z plot data in all unit slopes of hydraulic flow unit. To make sure that these equations provide a good permeability estimation, a comparison of permeability values and coefficient correlations between the calculated and measured permeabilities from hydraulic flow unit method with the other methods were considered, such methods are logarithm of permeability and porosity plot method and the Jorgensen (1988) method. Figure 4.7 shows a plot of logarithm of core determined permeability and porosity. The equation of Jorgensen method is defined as follows:

$$k = 84105\frac{\phi^{m+2}}{(1-\phi)^2} \tag{4.1}$$

where m is the cementation exponent.

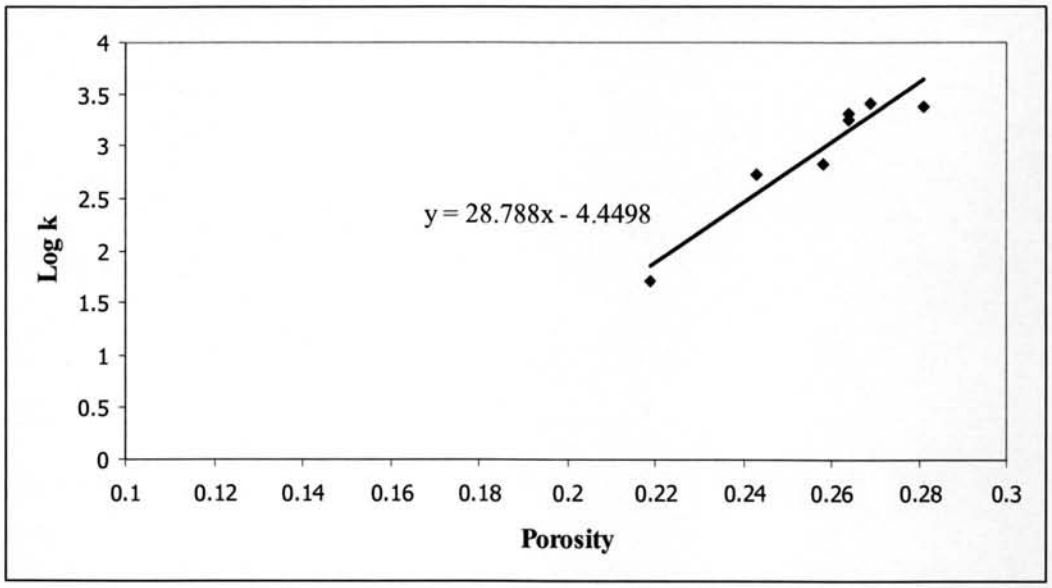

Figure 4.7: A plot of logarithm of permeability and porosity.

A plot of logarithm of permeability and porosity yields a linear relationship, its linear equation is quantified in Figure 4.7. Figure 4.8 shows the scatter plot between core permeability and calculated permeability of these methods. The comparison of coefficient correlations between HFU and the other methods is shown in Table 4.8, meanwhile permeability values are shown in Table 4.9.

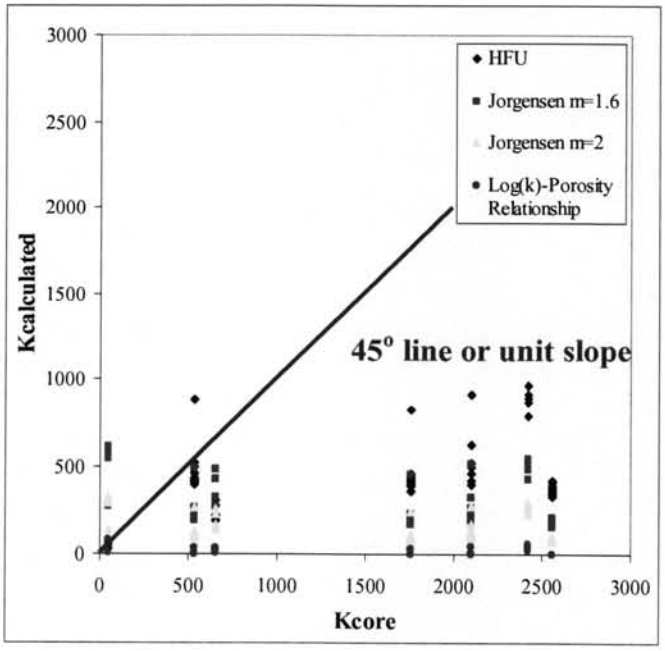

Figure 4.8: Scatter plot between core permeability and calculated permeability.

Table 4.8: Comparison of coefficient correlations between HFU and the other methods.

Method		Coefficeint Correlation
Hydraulic Flow Unit (HFU)		0.658
Jorgensen	m = 1.6	-0.345
	m = 2	-0.345
Log k = aΦ + b		-0.383

Table 4.9: Comparison of permeability values between HFU and the other methods.

Layer	Depth	Core Permeability (md)	Calculated Permeability (md)			
			HFU	Jorgensen m =1.6	Jorgensen m =2	Log (k) - Φ Plot Log k = aΦ+b
K2	1,620.5	658	309	480	256	37
			221	325	167	10
			191	273	138	6.2
			279	425	225	25
			191	273	138	6.2
			191	273	138	6.2
			279	425	225	25
			279	425	225	25
			191	273	138	6.2
			191	273	138	6.2
			191	273	138	6.2
			279	425	225	25
			191	273	138	6.2
			279	425	225	25
			221	325	167	10
			191	273	138	6.2
	1,626.2	2,420	915	509	274	45
			915	509	274	45
			870	480	256	37
			915	509	274	45
			786	425	225	25
			915	509	274	45
			915	509	274	45
			870	480	256	37
			893	494	265	41
			893	494	265	41
			915	509	274	45

Table 4.9: Comparison of permeability values between HFU and the other methods (continued).

Layer	Depth	Core Permeability (md)	Calculated Permeability (md)			
				Jorgensen		Log (k) - Φ Plot
			HFU	m=1.6	m=2	Log k = aΦ+b
K2	1,626.2	2,420	962	539	292	55
			786	425	225	25
			915	509	274	45
			915	509	274	45
			870	480	256	37
	1,636.0	51	53	605	331	82
			53	605	331	82
			53	605	331	82
			53	605	331	82
			48	539	292	55
			27	273	138	6.2
			53	605	331	82
			53	605	331	82
			50	571	311	67
			50	571	311	67
			50	571	311	67
			53	605	331	82
			50	571	311	67
			50	571	311	67
			50	571	311	67
			50	571	311	67
K3	1,646.2	2,100	624	325	167	10
			392	188	92	2.1
			498	249	125	4.7
			417	202	99	2.6
			498	249	125	4.7
			461	227	113	3.6
			517	261	131	5.4
			417	202	99	2.6
			384	184	89	2.0
			498	249	125	4.7
			498	249	125	4.7
			392	188	92	2.1
			417	202	99	2.6
			517	261	131	5.4
			417	202	99	2.6
			915	509	274	45
	1,646.6	533	461	227	113	3.6
			409	198	97	2.4
			517	261	131	5.4
			409	198	97	2.4
			461	227	113	3.6
			434	212	105	3.0

Table 4.9: Comparison of permeability values between HFU and the other methods (continued).

Layer	Depth	Core Permeability (md)	Calculated Permeability (md)			
			HFU	Jorgensen m=1.6	Jorgensen m=2	Log (k) - Φ Plot Log k = aΦ+b
K3	1,646.6	533	498	249	125	4.7
			417	202	99	2.6
			392	188	92	2.1
			461	227	113	3.6
			392	188	92	2.1
			417	202	99	2.6
			392	188	92	2.1
			461	227	113	3.6
			417	202	99	2.6
			885	489	262	39
	1,647.1	1,760	434	212	105	3.0
			384	184	89	2.0
			461	227	113	3.6
			384	184	89	2.0
			409	198	97	2.4
			417	202	99	2.6
			434	212	105	3.0
			417	202	99	2.6
			409	198	97	2.4
			417	202	99	2.6
			417	202	99	2.6
			361	171	82	1.6
			384	184	89	2.0
			443	217	107	3.2
			392	188	92	2.1
			827	452	240	30
	1,648.0	2,560	409	198	97	2.4
			346	163	78	1.4
			409	198	97	2.4
			332	155	74	1.3
			417	202	99	2.6
			384	184	89	2.0
			417	202	99	2.6
			361	171	82	1.6
			361	171	82	1.6
			369	175	85	1.7
			361	171	82	1.6
			346	163	78	1.4
			346	163	78	1.4
			384	184	89	2.0
			392	188	92	2.1
			417	202	99	2.6

In Figure 4.8 and Table 4.8, the correlation between the calculated and measured permeability from HFU shows the positive coefficient correlation of 0.658 while other methods provide the negative coefficient correlation in the range of -0.345 to -0.383. This can be inferred that permeability equations based on hydraulic flow unit provides a good estimation of permeability at uncored wells. The next section discusses the application of these permeability equations in reservoir simulation program. The cored measured permeability and porosity, the calculated permeability, and the simulated porosity will be used in reservoir simulation program by assuming different scenarios of input data.

4.3 Application of Permeability Equation

The permeability equations based on hydraulic flow unit was applied in reservoir simulation program (ECLIPSE) and the results of production profiles such as total production, recovery factor were observed. Three cases were assumed. The simulated porosity from two different realization maps and their corresponding permeability were used as inputs in case I and case II while case III the core measured permeability and porosity were used as inputs. The permeability and porosity values used in reservoir simulation program are shown in Table 4.10.

Table 4.10: Permeability and porosity for reservoir simulation program.

Layer	Depth (m)	Case I		Case II		Case III	
		Calculated Permeability (md)	Simulated Porosity	Calculated Permeability (md)	Simulated Porosity	Core Analysis	
						Permeability (md)	Porosity
K2	1,620.5	309	0.209	191	0.182	658	0.258
K2	1,626.2	915	0.212	786	0.203	2,420	0.281
K2	1,636.0	53	0.221	50	0.218	51	0.219
K3	1,646.2	624	0.19	392	0.166	2,100	0.264
K3	1,646.6	461	0.174	417	0.169	533	0.243
K3	1,647.1	434	0.171	361	0.162	1,760	0.264
K3	1,648.0	409	0.168	346	0.16	2,560	0.269

4.3.1 Reservoir Modeling

For this study, a black oil reservoir was selected for the oil field. It's developed by natural depletion. The production was simulated with one production well located at the center of reservoir, renamed "X02". The same area has been applied to reservoir modeling, but the thickness was considered only at the measured core interval. The schematic of the well and reservoir for this scenario is shown in Figure 4.9.

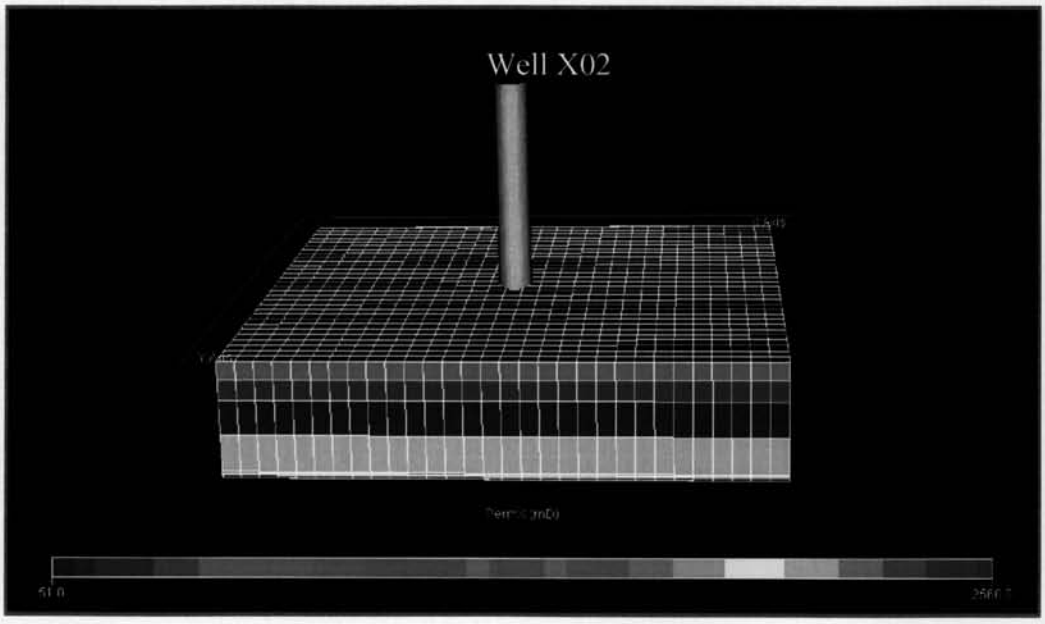

Figure 4.9: The schematic of wells and reservoir of the oil field.

4.3.2 Comparison the results

In this scenario, the production of black oil reservoir was simulated to produce by natural depletion method. The oil production rate was controlled at 7,000 stb/day in order to observe the production life, cumulative productions of oil, gas and water, recovery factor, and pressure. As shown in Figure 4.10, the oil production rate (FOPR) for case I, case II, and case III was kept constant as long as the reservoir can sustain such rate. Larger quantity of fluid contained in case III resulted in a longer oil production rate. The oil production total (FOPT) is shown in Figure 4.11. The oil production for case I, case II, and case III increased rapidly as far as the oil production

rate was kept constant at 7,000 stb/day. The oil production total was slightly increased while oil production rate was dropped. Figures 4.12 to 4.13 present the gas production rate (FGPR) and gas production total (FGPT) for case I, case II, and case III. Initially, gas production rate was almost unchanged at the rate of 3,000 Mscf/day approximately until reaching bubble point pressure (1,800 psia), it was increased steeply as long as the oil production rate kept constant. The drop in oil production rate caused the decline of gas production rate. The production gas can be produced until abandonment. The gas production total increased rapidly as long as it maintains an oil production rate of 7,000 stb/day. As soon as the oil production rate dropped, the gas production total was slightly increased. The water production rate (FWPR) and water production total (FWPT) for case I, case II and case III are illustrated in Figures 4.14 to 4.15. The water production rate was increased rapidly as long as the oil production rate kept constant and the drop of oil production rate caused the decline of water production rate. The water production total was increased rapidly as long as oil production rate kept constant. When the oil production rate was dropped, the water production total was slightly increased. As shown in Figure 4.16, the recovery factors (FOE) for case I, case II, and case III are not significant difference and fall in a narrow range of 0.207 to 0.229. The pressure profiles (FPR) for case I, case II and case III are shown in Figure 4.17. The pressure declined as the production of black oil reservoir kept on going onwards. A comparison results among case I, case II, and case III are shown in Table 4.11.

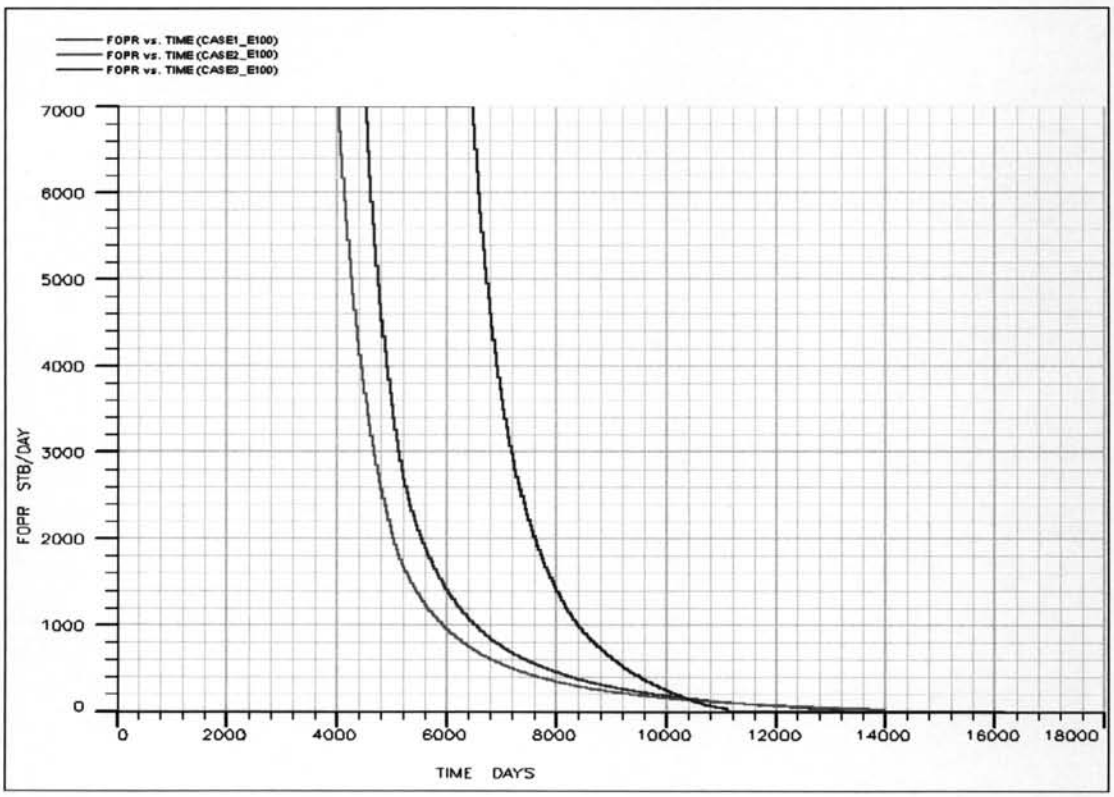

Figure 4.10: Oil production rate profiles (FOPR) for case I, case II, and case III.

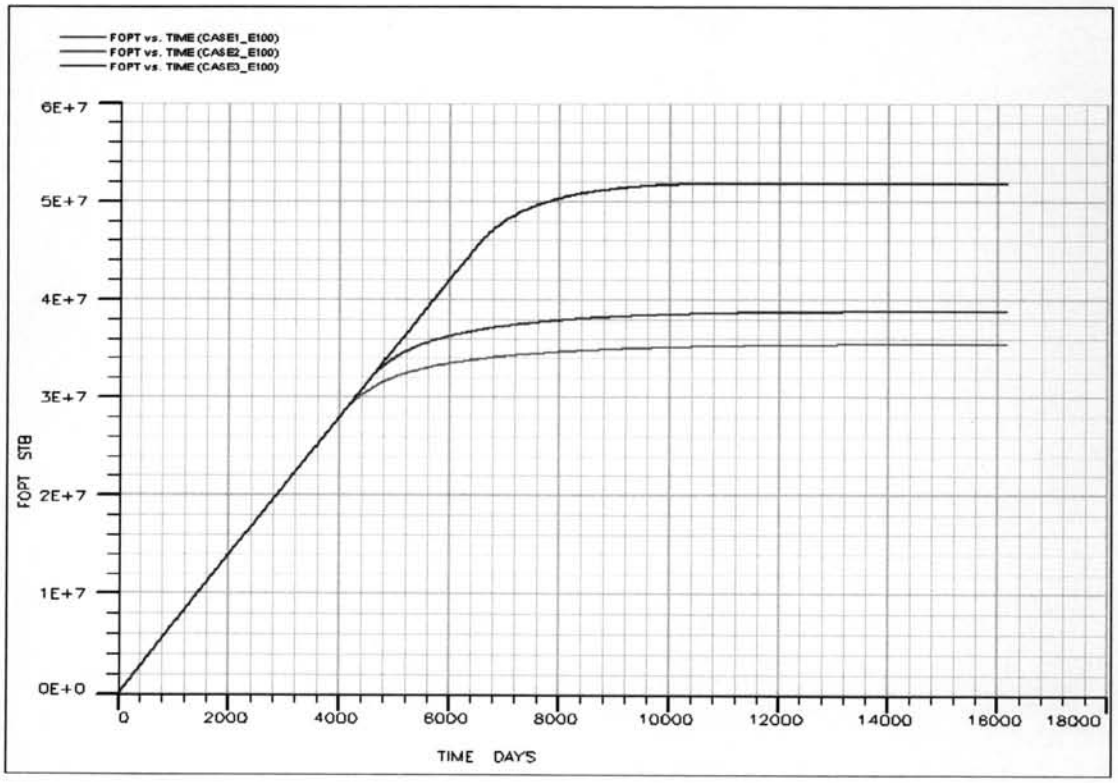

Figure 4.11: Total oil production profiles (FOPT) for case I, case II, and case III.

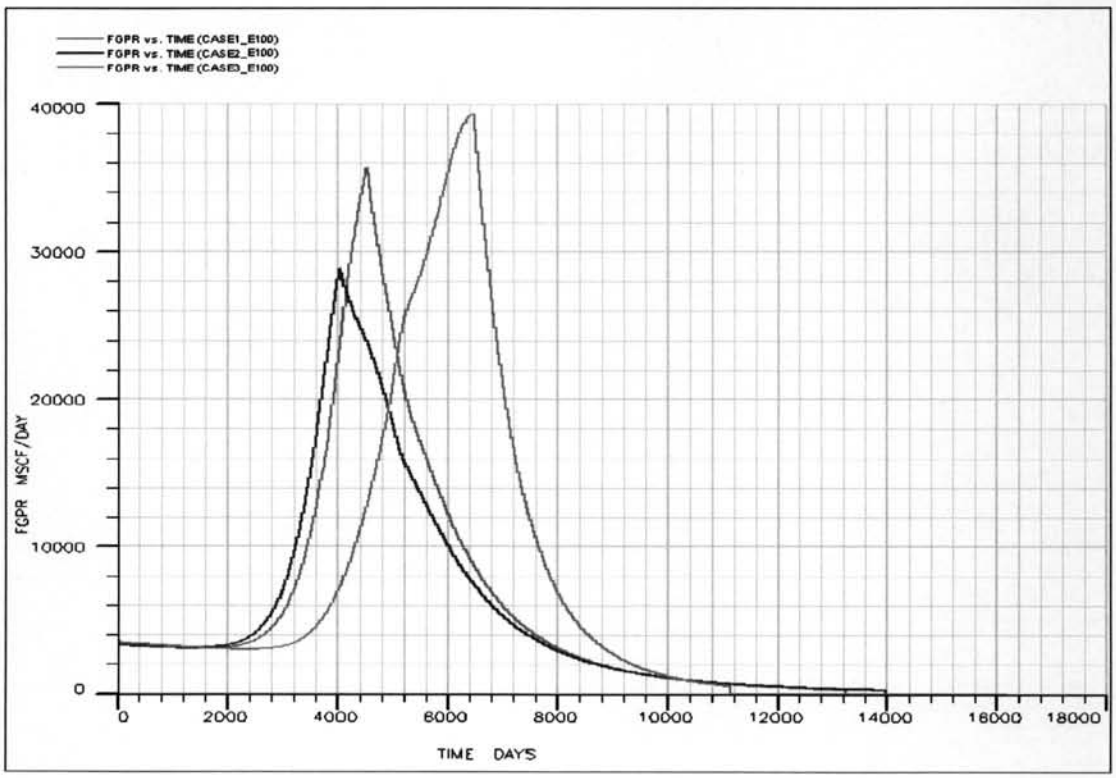

Figure 4.12: Gas production rate profiles (FGPR) for case I, case II and case III.

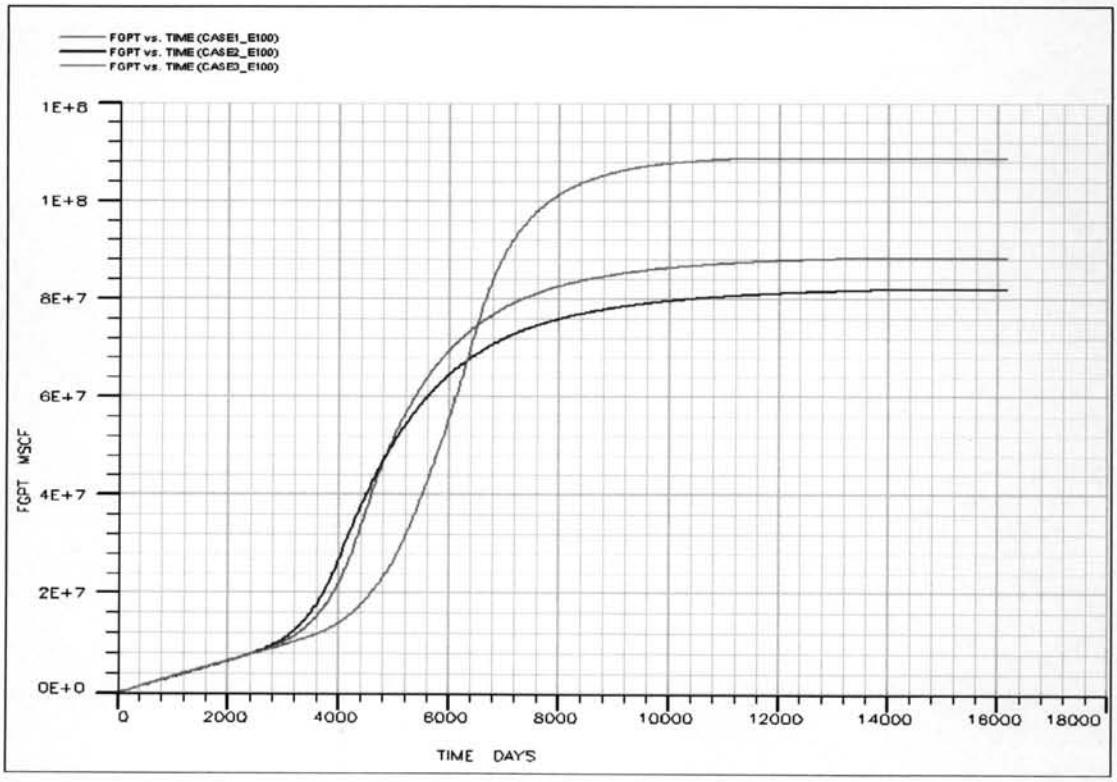

Figure 4.13: Total gas production profiles (FGPT) for case I, case II and case III.

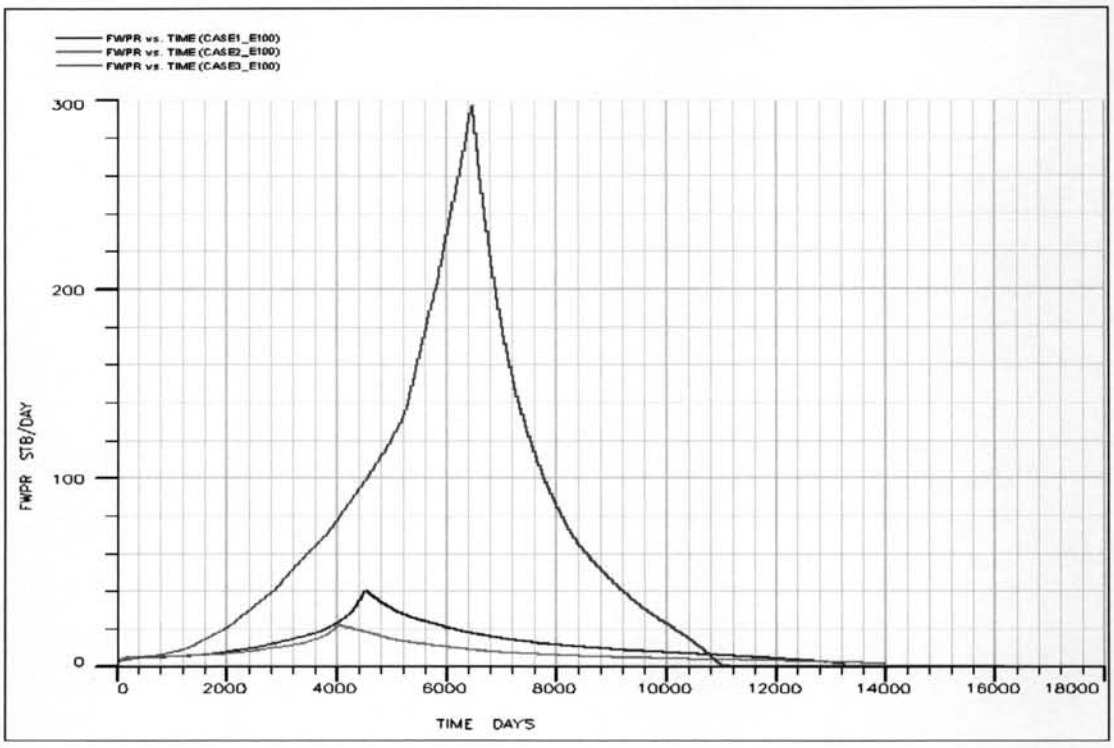

Figure 4.14: Water production rate profiles (FWPR) for case I, case II and case III.

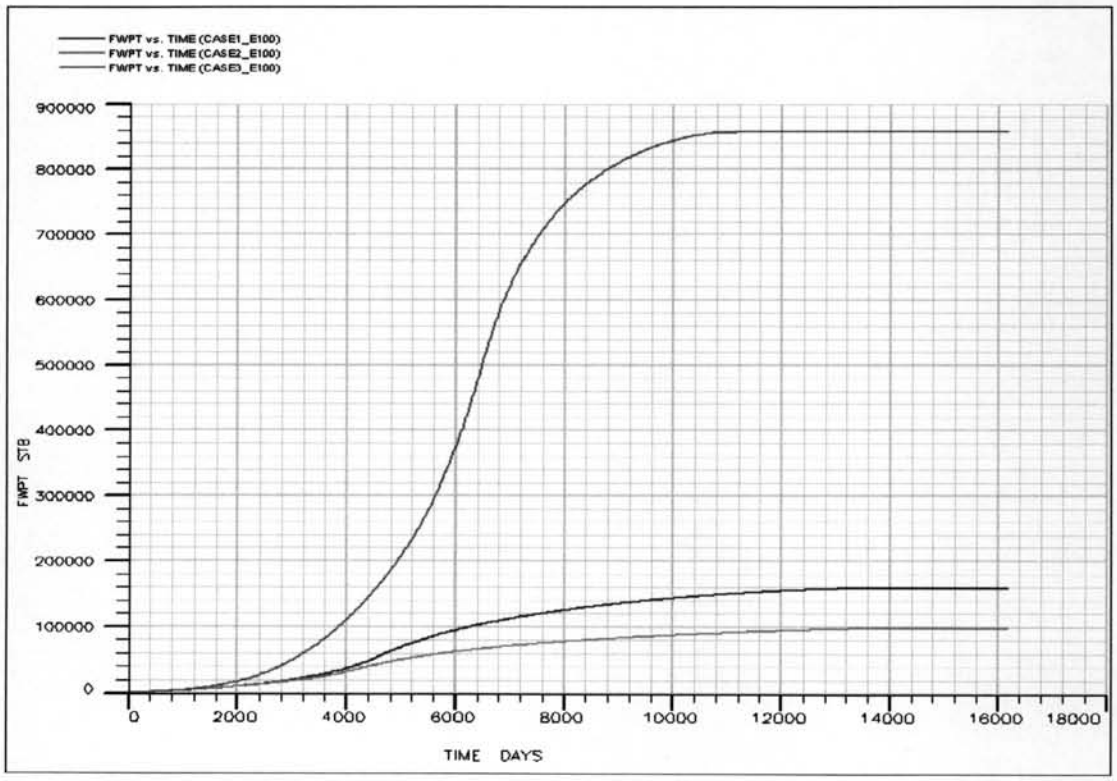

Figure 4.15: Total water production profiles (FWPT) for case I, case II, and case III.

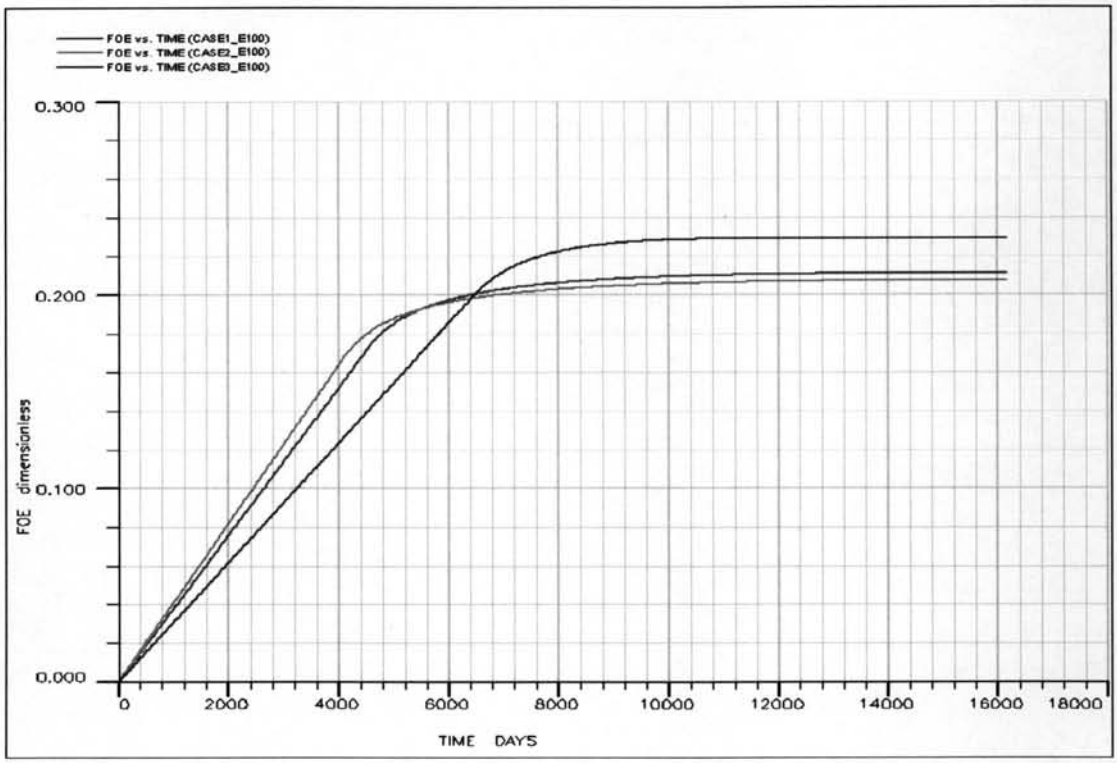

Figure 4.16: Recovery factor profiles (FOE) for case I, case II, and case III.

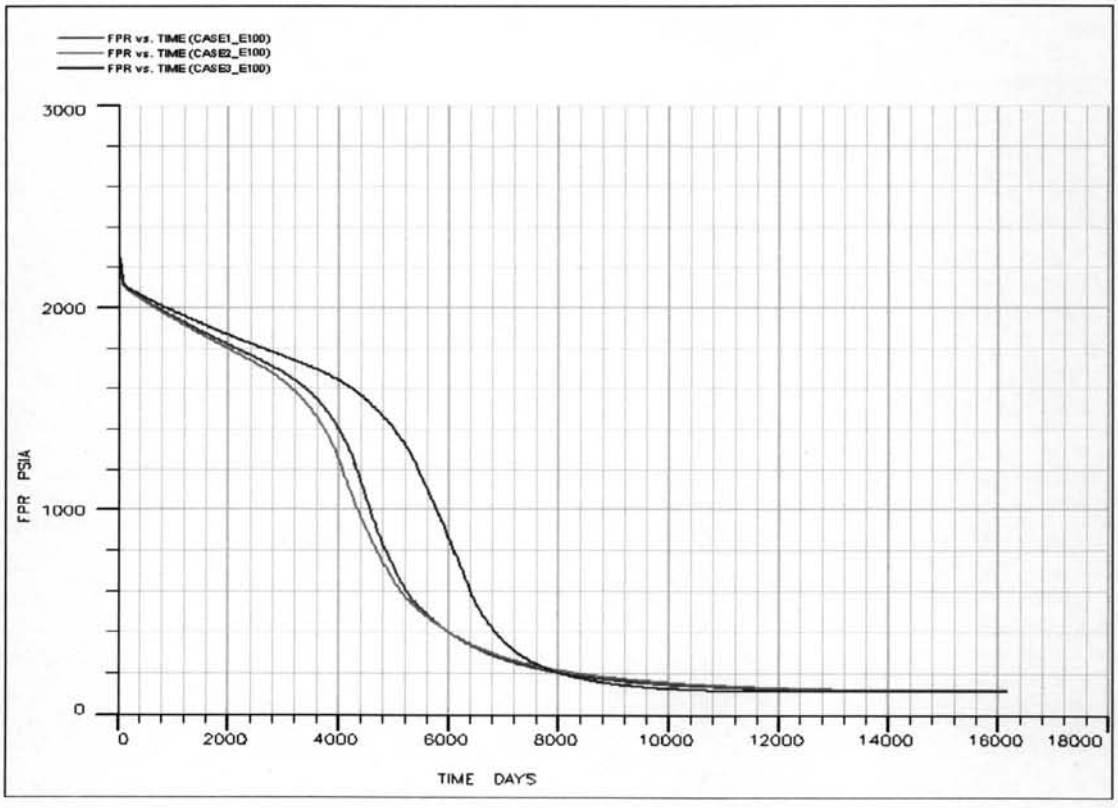

Figure 4.17: Pressure profiles (FPR) for case I, case II, and case III.

Table 4.11: Comparison results among case I, case II, and case III.

Summary	Case I	Case II	Case III
Total Production Time (Year)	36.28	38.20	30.52
Total Oil Production (STB)	38,763,416	35,389,280	51,820,656
Total Gas Production (Mscf)	88,209,472	81,856,072	108,567,000
Total Water Production (STB)	158,005	98,349	857,638
OOIP (STB)	183,815,460	170,716,000	226,249,760
Recovery Factor (%)	21.09	20.73	22.90

Observed from Figures 4.10 to 4.17 and Table 4.11, the results in case I and case II are almost similar. It indicates that the idea of incorporating simulated porosity values in permeability equations that is able to estimate permeability efficiently in this oil field. However, there is a remarkable contrast among case I, case II, and case III, in term of total water production. Whereby, case III indicates quite different total water production to cases I and case II due to larger permeability and porosity inputs in case III.

Although the permeability equations in this oil field can be obtained directly from porosity and permeability in core analysis, only a few samples are available in practice. The ability of geostatistical simulation to provide many equal probable realization maps was proved benefit for this study. Where the porosity was simulated throughout the field, and these maps were used as an additional input data in determining permeability equations. In overall, the permeability equations based on hydraulic flow unit provide a good estimation of permeability at uncored wells for this oil field.